

Isotope shifts of energy levels in the naturally abundant isotopes of strontium and calcium

C.-J. Lorenzen and K. Niemax

Institut für Experimentalphysik, Universität Kiel, D-2300 Kiel 1, Federal Republic of Germany

L. R. Pendrill

Fysiska Institutionen, Chalmers Tekniska Högskola, S-412 96 Göteborg, Sweden

(Received 23 July 1982)

The isotope shifts of long series of spectral lines in the optical spectra of the alkaline-earth elements Ca and Sr have been measured by Doppler-free, two-photon laser spectroscopy with a thermionic diode. The variation of transition isotope shifts with transition energy yields the *level* isotope shifts with reference to the ionization limit and how these shifts vary with the binding energy of the optically active electron. The largest isotope shifts of levels in these elements appear to arise from the specific-mass effect in the presence of state mixing.

I. INTRODUCTION

Optical isotope shifts in atomic spectra have been studied for many years, mainly with the aim of obtaining information on the size and shape of the nuclear charge distribution. In some cases, for example, for highly unstable radioactive nuclei, their study is the only way, at present, of measuring the nuclear size.¹

Optical isotope shifts are small differences in the total energy of one isotope with respect to another arising from the effects of different nuclear charge distributions (volume shift) and nuclear masses (mass shift) on the energy of the optically active electron. The energy of the optical electron may also be influenced by the other atomic electrons. Nuclear information may therefore be extracted from optical isotope shifts only after one has accurately accounted for the influences from many-electron interactions on the atomic spectra.

In this paper we report the results of extensive measurements of isotope shifts along long series of optical transitions in the alkaline-earth elements Ca and Sr. The optical spectra of these elements, which are the subject of much current experimental and theoretical interest,²⁻⁵ reflect the motions of the two valence electrons about the nucleus and inert-gas-like core. Both valence electrons may be optically excited and may interact with each other. Our measurements, in which one electron is excited with light progressively further and further from the rest of the atom, reveal the varying influences of the atom on the optically active electron.

For sufficiently highly excited states, this electron is shown to have no isotope shift, apart from the Bohr mass shift. This enables level isotope shifts, due to the optical electron (but including influences by the rest of the atomic electrons), to be given with reference to the ionization limit where that electron is at rest at infinity (Ritschl and Schober⁶ in 1937, Bradley and Kuhn⁷ in 1951, Niemax and Pendrill⁸ in 1980). For lower-lying states, there are increasing isotope shift contributions as the excited electron approaches the core. Where a level of another configuration comes close in energy to the directly excited series, the level shifts are observed to change abruptly.

Level isotope shifts are of more direct theoretical interest than transition shifts. Recently, Mårtensson and Salomonson⁹ calculated, with some success, specific mass shifts in Li and K for states whose level shifts had been measured.⁸ They started the calculation with a central-field (Hartree-Fock) description of the alkali-metal ionic core (which is inert-gas-like and thus spherically symmetric). The isotope shift contributions from the valence electron (including its influence on the core) of the neutral alkali-metal atom could then be calculated by many-body perturbation theory. This gave directly the level isotope shifts relative to the atom's ionization limit.

The present measurements give level shifts in the neutral alkaline earths with reference to the ground state of the first ion. Measurements on transitions to highly excited states of this ion would enable the level shifts to be related to the inert-gas-like second

ion. This state is a better choice of reference level for the isotope shifts than is a state of the first, alkali-metal-like ion, owing to its great binding energy and sphericity.

So as to ensure that many-electron effects are absent and that the highly excited state really has zero isotope shift relative to the ionization limit, we employ a method used earlier⁸ for K and Li in which transition isotope shifts are measured for at least two series converging to the same ionization limit. The total transition shifts are plotted against the transition energy. Also plotted is a straight line corresponding to the Bohr mass shift (BMS), calculated from the expression, $-(m/M)E$, for the Bohr mass shift of an level of binding energy E , in an isotope of mass M , relative to an infinitely heavy isotope. When the different series of transition isotope shifts have converged on to a straight line parallel to the Bohr mass shift, then the upper level of each transition has zero residual shift (i.e., non-BMS) with respect to the ionization limit. The shift of the lower level of the transitions is given simply by the difference from the Bohr mass shift straight line of the transition shifts to states with zero residual shift.

II. EXPERIMENT

The broad, high-resolution spectral coverage required in this experiment was provided by the use of a combination of Doppler-free, two-photon excitation of the alkaline-earth atoms with light from a single-mode, tunable dye laser and detection with the sensitive thermionic diode which has been widely employed in the last years. Details of the experimental setup may be found, for example, in the earlier publications of the present authors^{8,10}. In this article we merely recall the salient features.

A stainless-steel heat-pipe thermionic diode with a shielding grid was filled with the naturally abundant isotopes of the alkaline-earth elements (Ca and Sr). The cathode filament of the diode was directly heated to a temperature at which the diode current was limited by space charge. No voltage bias was applied across the diode. Neon was used as a buffer gas (100 mTorr at room temperature) since it is known¹¹ to have the smallest collisional cross sections of the inert gases for the broadening and shift of the metal atom lines.

Light from a frequency-stabilized cw ring dye laser (Spectra-Physics 380D) was focused and retroreflected through the heat-pipe cell. Ion signals, resulting from collisional ionization of the alkaline-earth atoms following Doppler-free, two-photon excitation, were taken from the heat-pipe wall and fed into a lock-in amplifier. Typical spectra, recorded as the dye laser was electronically tuned through

each resonance, are displayed in Figs. 1 and 4.

In strontium, the two-photon transitions $5s^2^1S_0$ to $5s5d^1D_2$ and to $5s5d^3D_2$ were excited with laser light powers of up to 300 mW from the laser dye Rhodamine 6G. For excitation of the transition from the ground state to $5s6s^1S_0$ the dye Rhodamine-640 was used, whereas the transitions to the states $5sns^1S_0$ ($10 \leq n \leq 33$), to $5snd^1D_2$ ($9 \leq n \leq 60$), and to $5snd^3D_2$ ($13 \leq n \leq 18, n=30$) were excited with blue laser light from the dye Stilbene 3, with typical laser powers of between 30 and 150 mW.

In calcium, the two-photon transitions $4s^2^1S_0$ to $4sns^1S_0$ ($7 \leq n \leq 10$), to $4snd^1D_2$ ($6 \leq n \leq 8$), and to the $3d5s$ ($J=2$) perturber state were excited with laser light from the dye Stilbene 3, while the ground state to $4s11s^1S_0$ transition was excited with laser light from Stilbene 1. Unfortunately, no other transitions could be investigated with this dye because the low laser power (15 mW at most) did not allow proper locking of the laser frequency.

Frequency intervals in the two-photon spectra were measured relative to the interference fringes produced when part of the laser light passed through a calibrated confocal etalon of 147.5-MHz-free spectral range. During each spectral scan, thermal drifts of the etalon could be neglected. The uncertainties in the measured frequency intervals (typically 4–6 MHz) were due to the statistical errors of the measurements and to nonlinearities in the laser scan which caused systematic uncertainties in the interpolation of the free spectral ranges of the etalon. An independent check of the measured isotope shift intervals was made by using our high-precision vacuum wavelength meter¹² to measure the wavelength of each spectral component to a relative precision of 3×10^{-9} . The wavelength meter data were always within the cited error bars of the data measured with the etalon. Since each atomic resonance occurred with the absorption of two photons, the frequency intervals on the atomic spectra were exactly one-half of the transition frequency intervals.

The spectral widths of the observed two-photon transitions were about 3–5 MHz, due to twice the laser linewidth (of nearly 1 MHz), together with some self-broadening and neon-gas broadening.

III. EXPERIMENTAL RESULTS

In this section we present the results obtained by the above-described technique for extracting level isotope shifts in the alkaline-earth elements Ca and Sr relative to their alkali-metal-like ions. A positive level shift is defined as one in which the binding energy is greater in the heavier isotope.

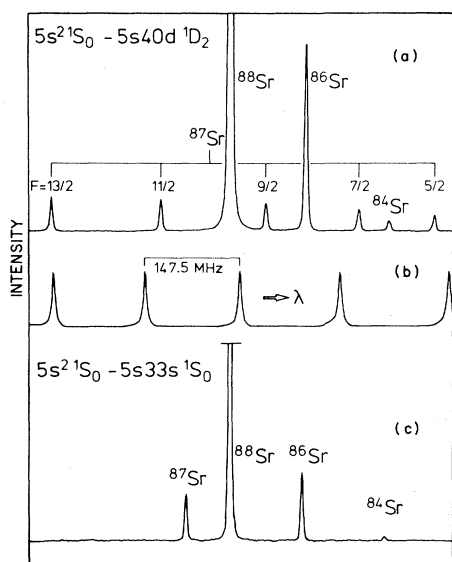


FIG. 1. Spectral scans of the two-photon transitions $5s^2\ ^1S_0$ to $5s40d\ ^1D_2$ and to $5s33s\ ^1S_0$ in strontium. Frequency markers from a 147.5-MHz FSR etalon are also shown.

A. Strontium

Figure 1 shows an example of two spectral scans for the transitions from the ground state $5s^2\ ^1S_0$ to the states $5s40d\ ^1D_2$ and to $5s33s\ ^1S_0$ in Sr, in the measurements performed at Kiel. Isotope shifts and hyperfine structures were measured relative to a calibrated Fabry-Perot etalon, whose interference fringes are also shown in Fig. 1.

In Fig. 2 we plot the transition isotope shifts (TIS) as a function of transition energy for three series of spectral lines, corresponding to transitions from $5s^2\ ^1S_0$ to $5sns\ ^1S_0$, $5snd\ ^1D_2$, and $5snd\ ^3D_2$ ($5 \leq n \leq 60$). Also plotted is the BMS for the three pairs of isotopes ^{88}Sr - ^{87}Sr , ^{88}Sr - ^{86}Sr , and ^{88}Sr - ^{84}Sr (shown as solid straight lines in Fig. 2).

The even-even transition isotope shifts show a relatively simple dependence on transition energy. The TIS of the 1S_0 states lie on a straight line (dashed in Fig. 2) parallel to, but shifted from, the BMS. The 1D and 3D TIS, however, are varying in a more complex way, exhibiting especially a configuration mixing perturbation in the isotope shifts near $n=15$ and 16, caused by a crossing of the singlet and triplet series which is known to occur from earlier energy level measurements. Higher members of the 1D series can be seen to have TIS which converge monotonically on to the same straight line as the 1S series. When this convergence of the different series of isotope shifts occurs (within the error bars), then

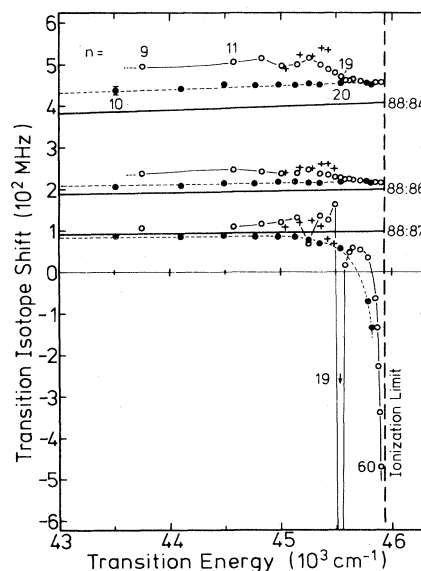


FIG. 2. Transition isotope shifts in strontium vs transition energies above $43\ 500\ \text{cm}^{-1}$ to the ionization limit. \bullet : $5s^2\ ^1S_0$ to $5sns\ ^1S_0$, \circ : $5s^2\ ^1S_0$ to $5snd\ ^1D_2$, $+$: $5s^2\ ^1S_0$ to $5snd\ ^3D_2$.

the residual level isotope shift (RLIS) of the upper level of each transition is zero, despite a still varying quantum defect.

The constant deviation between the dashed and BMS lines in Fig. 2 gives the RLIS of the ground state $5s^2\ ^1S_0$ relative to the ionization limit of Sr I, i.e., the ground state $5s_{1/2}$ of the Sr II alkali-metal-like ion of the even isotopes. This RLIS, together with the RLIS of other levels of the Sr atom connected through measured transitions with the neutral atom ground state, are presented in Table I. We use the transition isotope shift measurements of Heilig¹⁴ in order to obtain the level shifts of the first excited 1P state.

All states tabulated, apart from the ground state and the state $5s5p\ ^1P_1$ of Sr, can be seen to have predominantly specific mass isotope shifts between the even isotopes: The RLIS of the isotope pair ^{88}Sr - ^{84}Sr are twice those of the pair ^{88}Sr - ^{86}Sr , within the error bars, reflecting the differences in mass between the isotope pairs. Some volume effect is apparent in both the ground state and the first excited 1P_1 state, although how much specific mass and volume effects are present cannot be estimated without some theoretical work or measurement (in muonic atoms, e.g.) of states where the specific mass shift (SMS) can be shown to be zero.

The spectrum of the isotope ^{87}Sr is profoundly affected by hyperfine interaction resulting from the nonzero nuclear spin of that isotope. In the vicinity

TABLE I. Transition isotope shifts (TIS) and residual level isotope shifts (RLIS) in Sr I. Reference level: $5s_{1/2}$ ground state of Sr II.

Transition	TIS (MHz)			Level	RLIS (MHz)		
	$^{88}\text{Sr}-^{87}\text{Sr}$	$^{88}\text{Sr}-^{86}\text{Sr}$	$^{88}\text{Sr}-^{84}\text{Sr}$		$^{88}\text{Sr}-^{87}\text{Sr}$	$^{88}\text{Sr}-^{86}\text{Sr}$	$^{88}\text{Sr}-^{84}\text{Sr}$
$5s^2\ ^1S_0 \rightarrow 5sns\ ^1S_0$				$5sns\ ^1S_0$			
				$5s^2$	-9(3)	+18(2)	+48(3)
$5s\ 6s$	~0(8)	+161(6)		$5s\ 6s$	+57(10)	-10(7)	
$5s\ 10s$	+87(6)	+206(8)	+438(10)	$5s\ 10s$	0(9)	0(8)	0(8)
$5s\ 11s$	+85	+208	+437	$5s\ 11s$	0	0	0
$5s\ 12s$	+88	+214	+453	$5s\ 12s$	0	0	0
$5s\ 13s$	+85	+212	+449	$5s\ 13s$	0	0	0
$5s\ 14s$	+83	+217	+450	$5s\ 14s$	+6	0	0
$5s\ 15s$	+83	+217	+450	$5s\ 15s$	+6	0	0
$5s\ 16s$	+77	+215	+455	$5s\ 16s$	+11	0	0
$5s\ 17s$	+68	+213	+450	$5s\ 17s$	+20	0	0
$5s\ 20s$	+56	+217	+454	$5s\ 20s$	+33	0	0
$5s\ 30s$	-72	+218	+455	$5s\ 30s$	+161	0	0
$5s\ 33s$	-133	+214	+452	$5s\ 33s$	+222	0	0
$5s^2\ ^1S_0 \rightarrow 5snd\ ^1D_2$				$5snd\ ^1D_2$			
$5s\ 5d$	+135(6)	+302(5)	+642(9)	$5s\ 5d$	-69(9)	-133(7)	-285(12)
$5s\ 9d$	+106(10)	+237(8)	+496(8)	$5s\ 9d$	-21(13)	-29(10)	-59(11)
$5s\ 11d$	+109	+245	+506	$5s\ 11d$	-22	-33	-61
$5s\ 12d$	+116	+242	+515	$5s\ 12d$	-29	-29	-68
$5s\ 13d$	+118	+237	+496	$5s\ 13d$	-30	-23	-47
$5s\ 14d$	+130	+238	+500	$5s\ 14d$	-42	-24	-50
$5s\ 15d$	+70	+246	+516	$5s\ 15d$	+18	-31	-65
$5s\ 16d$	+136	+236	+499	$5s\ 16d$	-48	-21	-47
$5s\ 17d$	+125	+234	+487	$5s\ 17d$	-37	-18	-35
$5s\ 18d$	+162	+229	+481	$5s\ 18d$	-74	-13	-28
$5s\ 19d$	~ -1500	+227	+471	$5s\ 19d$	~ +1500	-11	-18
$5s\ 20d$	+16	+222	+462	$5s\ 20d$	+73	-6	-8
$5s\ 21d$	+47	+227	+462	$5s\ 21d$	+42	-11	-8
$5s\ 22d$	+58	+223	+466	$5s\ 22d$	+31	-7	-12
$5s\ 25d$	+53	+219	+460	$5s\ 25d$	+36	-2	-5
$5s\ 30d$	+35	+217	+453	$5s\ 30d$	+54	0	0
$5s\ 40d$	-64	+219	+455	$5s\ 40d$	+153	0	0
$5s\ 45d$	-133	+218	+453	$5s\ 45d$	+222	0	0
$5s\ 50d$	-227	+215	+456	$5s\ 50d$	+316	0	0
$5s\ 55d$	-338	+216	+453	$5s\ 55d$	+427	0	0
$5s\ 60d$	-469	+211	+454	$5s\ 60d$	+559	0	0
$5s^2\ ^1S_0 \rightarrow 5snd\ ^3D_2$				$5snd\ ^3D_2$			
$5s\ 5d$	+94(5)	+216(6)	+446(6)	$5s\ 5d$	-28(8)	-46(8)	-86(9)
$5s\ 13d$	+108(10)	+241(8)	+490(8)	$5s\ 13d$	-20(13)	-27(10)	-41(11)
$5s\ 14d$	+119	+252	+523	$5s\ 14d$	-31	-38	-73
$5s\ 15d$	+125	+248	+519	$5s\ 15d$	-37	-33	-68
$5s\ 16d$	+108	+258	+541	$5s\ 16d$	-20	-43	-89
$5s\ 17d$	+79	+260	+536	$5s\ 17d$	+9	-45	-84
$5s\ 18d$	+68	+247	+455	$5s\ 18d$	+21	-31	
$6s\ 30d$		+218	+455	$5s\ 30d$		0	0
$5s^2\ ^1S_0 \rightarrow 5s\ 5p\ ^1P_1$		+126(6) ^a	+258(15) ^a	$5s\ 5p\ ^1P_1$		-14(6)	-17(15)

^aReference 14.

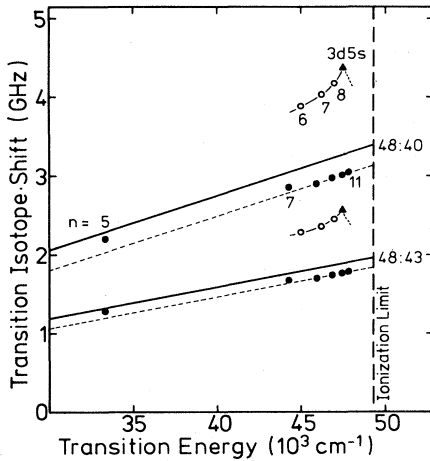


FIG. 3. Transition isotope shifts in calcium vs transition energies above $30\,000\text{ cm}^{-1}$ to the ionization limit. Only the shifts between the isotopes ^{40}Ca , ^{43}Ca and ^{48}Ca are shown to avoid overcrowding of the plot. ●: $4s^2\ ^1S_0$ to $4sns\ ^1S_0$, ○: $4s^2\ ^1S_0$ to $4snd\ ^1D_2$, ▲: $4s^2\ ^1S_0$ to $3d\ 5s$ ($J=2$).

of the crossing in energy of two series of energy levels, configuration mixing of the hyperfine interaction may result in shifted and distorted hyperfine structure for the odd isotope (Kopfermann¹⁵). The hyperfine structure of all $5snd\ ^1D_2$ states at and below $n=15$ are inverted. Higher 1D states show the normal structure (as exemplified in Fig. 1). The centroids of the hyperfine structures of the per-

turbed states of the ^{88}Sr isotope were observed to be also shifted from the energy they would have in the absence of the nuclear spin. In particular, a strong shift of the $19\ ^1D_2$ level of ^{87}Sr caused by the near coincidence in energy of this state with the $19\ ^3D_3$ state was observed. The convergence of singlet and triplet states for each orbital angular momentum approaching the ionization limit of ^{87}Sr caused, through hyperfine mixing, a strongly diverging series of shifts of the highly excited states of that isotope. These purely hyperfine-mixing effects, which have been independently measured and analyzed by Beigang and co-workers^{3,16} mask the true isotope shifts and will not be discussed further here.

Away from the regions of configuration mixing, however, it is possible to extract level isotope shifts involving the odd isotope with a fairly simple approach. At the ionization limit, all interactions involving the optically active electron vanish, since there the electron is at rest at infinity. If we then calculate the difference in ionization limits of, say, the $5sns\ ^1S_0$ series of energy levels of the isotopes ^{87}Sr and ^{88}Sr (as measured recently by Beigang *et al.*¹⁷) and subtract the hyperfine energy of the remaining $5s$ electron, and the BMS, we should obtain the residual level isotope shift of the Sr I ground state for that isotope pair. The result is $-13(30)$ MHz. This value of the ground-state RLIS is confirmed by examining another spectral region away from configuration mixing: The even-odd residual

TABLE II. Transition isotope shifts (TIS) in Ca I.

Transition	Transition isotope shift (MHz)				
	$^{48}\text{Ca}-^{46}\text{Ca}$	$^{48}\text{Ca}-^{44}\text{Ca}$	$^{48}\text{Ca}-^{43}\text{Ca}$	$^{48}\text{Ca}-^{42}\text{Ca}$	$^{48}\text{Ca}-^{40}\text{Ca}$
$4s^2\ ^1S_0-4s\ 5s\ ^1S_0^a$		+ 1023.5(3)	+ 1287.2(3)	+ 1587.2(3)	+ 2193.5(3)
$4s\ 7s\ ^1S_0^b$		+ 1330(8)	+ 1671(8)	+ 2059(10)	+ 2846(10)
$4s\ 8s\ ^1S_0^b$		+ 1347(8)	+ 1696(8)	+ 2091(10)	+ 2887(10)
$4s\ 9s\ ^1S_0^b$		+ 1385(8)	+ 1745(8)	+ 2152(10)	+ 2976(10)
$4s\ 10s\ ^1S_0^b$	+ 669(6)	+ 1404(8)	+ 1766(8)	+ 2181(8)	+ 3020(10)
$4s\ 11s\ ^1S_0^b$		+ 1415(8)	+ 1781(8)	+ 2197(10)	+ 3040(10)
$4s\ 4p\ ^1P_1^c$	+ 342(6)	+ 734(6)	+ 899(6)	+ 1117(6)	+ 1506(3)
$4s\ 4p\ ^3P_1^d$	+ 441(2)	+ 926(1)	+ 1140(2)	+ 1413(1)	+ 1923(1)
$4s\ 6d\ ^1D_2^b$		+ 1810(8)	+ 2281(8)	+ 2812(10)	+ 3882(10)
$4s\ 7d\ ^1D_2^b$		+ 1876(8)	+ 2355(8)	+ 2914(10)	+ 4031(10)
$4s\ 8d\ ^1D_2^b$		+ 1942(8)	+ 2450(8)	+ 3016(10)	+ 4164(10)
$3d\ 5s\ (J=2)^b$	+ 970(8)	+ 2031(8)	+ 2566(8)	+ 3154(10)	+ 4367(10)
$4s\ 4p\ ^3P_2-4s\ 5s\ ^3S_1^e$			- 78(5)		- 116(4)

^aPalmer *et al.*, Ref. 5.

^bThis work.

^cBrandt *et al.*, Ref. 19.

^dBergmann *et al.*, Ref. 20.

^eGrundevik *et al.*, Ref. 4.

TABLE III. Residual level isotope shifts (RLIS) and their separation into specific mass shifts (SMS) and field shifts (FS) in Ca I. Reference level: $5s_{1/2}$ ground state of Sr II. All values in MHz.

Level		$^{48}_{20}\text{Ca}-^{46}_{20}\text{Ca}$	$^{48}_{20}\text{Ca}-^{44}_{20}\text{Ca}$	$^{48}_{20}\text{Ca}-^{43}_{20}\text{Ca}$	$^{48}_{20}\text{Ca}-^{42}_{20}\text{Ca}$	$^{48}_{20}\text{Ca}-^{40}_{20}\text{Ca}$
$4s^2\ ^1S_0$	RLIS	-39(8)	-76(5)	-124(6)	-144(6)	-236(8)
	SMS	-51(4)	-107(4)	-137(5)	-169(5)	-236(8)
	FS	+12(9)	+31(5)	+13(8)	+25(8)	0
$4s\ 5s\ ^3S_1$	RLIS			+89(9)		+113(9)
	SMS			+66(6)		+113(9)
	FS			+23(11)		0
$4s\ 4p\ ^1P_1$	RLIS	-28(10)	-72(8)	-80(10)	-102(9)	-120(9)
	SMS	-26(4)	-55(5)	-70(6)	-86(6)	-120(9)
	FS	-2(12)	-17(10)	-10(12)	-16(12)	0
$4s\ 4p\ ^3P_1$	RLIS	-253(8)	-528(5)	-658(9)	-812(8)	-1116(8)
	SMS	-243(4)	-508(4)	-648(5)	-797(5)	-1116(8)
	FS	-10(9)	-20(7)	-10(10)	-15(9)	0
$4s\ 5s\ ^1S_0$	RLIS		-60(5)	-82(8)	-98(8)	-143(8)
	SMS		-65(5)	-83(5)	-102(6)	-143(8)
$4s\ 7s\ ^1S_0$	RLIS		-25(10)	-30(12)	-34(13)	-46(13)
	SMS		-21(7)	-27(7)	-33(9)	-46(13)
$4s\ 8s\ ^1S_0$	RLIS		+8(10)	+9(12)	+13(13)	+23(13)
	SMS		+10(7)	+13(7)	+16(9)	+23(13)
$4s\ 9s\ ^1S_0$	RLIS		0(10)	0(12)	0(13)	0(13)
$4s\ 10s\ ^1S_0$	RLIS	0(8)	0(10)	0(10)	0(10)	0(12)
$4s\ 11s\ ^1S_0$	RLIS		0(10)	0(12)	0(13)	0(13)
$4s\ 6d\ ^1D_2$	RLIS		-483(10)	-611(12)	-752(13)	-1033(13)
	SMS		-470(7)	-600(7)	-738(9)	-1033(13)
$4s\ 7d\ ^1D_2$	RLIS		-511(10)	-637(12)	-795(13)	-1099(13)
	SMS		-500(7)	-639(7)	-785(9)	-1099(13)
$4s\ 8d\ ^1D_2$	RLIS		-554(10)	-702(12)	-860(13)	-1181(13)
	SMS		-537(7)	-686(7)	-843(9)	-1181(13)
$3d\ 5s\ (J=2)$	RLIS	-301(10)	-627(10)	-798(12)	-973(13)	-1349(13)
	SMS	-293(7)	-614(7)	-784(7)	-963(9)	-1349(13)

isotope shifts of transitions to the $5sns\ ^1S_0$ ($10 \leq n \leq 13$) were found to be constant (within the error bars) as a function of the transition energy, as may be seen from Fig. 2. These transitions have isotope shifts deviating by $-9(3)$ MHz from the BMS.

In Table I we list the values of the RLIS for the isotope pair $^{88}\text{Sr}-^{87}\text{Sr}$ derived from the above value of the ground-state shift. The specific mass effect for the isotope pair $^{88}\text{Sr}-^{87}\text{Sr}$ may be calculated from

those even-even shifts shown above to be pure mass shifts by multiplying the latter by the appropriate mass factor (viz., the SMS in the pair $^{88}\text{Sr}-^{87}\text{Sr}$ is half the SMS in $^{88}\text{Sr}-^{86}\text{Sr}$). The level shifts for $^{88}\text{Sr}-^{87}\text{Sr}$ for most states appear to be at least 50% specific mass shift, apart from the ground state (where there is some volume effect) and those states most strongly affected by hyperfine mixing. The $5s\ 5d\ ^1D_2$ and 3D_2 states, for example, appear to

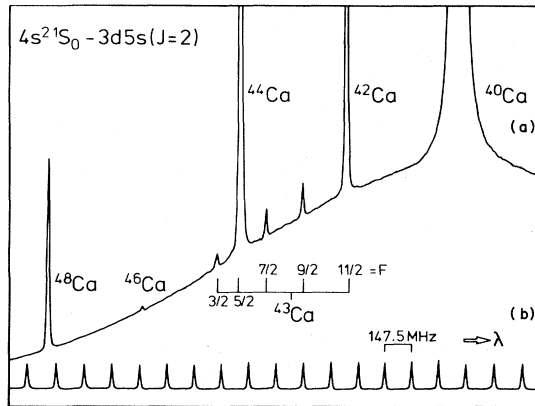


FIG. 4. Spectral scan of the two-photon transition from the ground state $4s^2\ ^1S_0$ to the perturber state $3d\ 5s$ ($J=2$) in calcium. Frequency markers from a 147.5-MHz FSR etalon are also shown. Note that the natural abundances of ^{46}Ca and ^{40}Ca are 0.0033% and 96.97%, respectively.

have purely specific mass shifts (within the error bars), even for the isotope pair ^{88}Sr - ^{87}Sr .

B. Calcium

Similar systematic measurements were made of transition isotope shifts along several series of energy levels converging to the first ionization limit of the naturally abundant isotopes of calcium. Figure 3 shows part of a plot of TIS versus transition energy for just two pairs of isotopes, ^{48}Ca - ^{40}Ca and ^{48}Ca - ^{43}Ca , for the transitions $4s^2\ ^1S_0$ to $4sns\ ^1S_0$ ($5 \leq n \leq 11$) and $4snd\ ^1D_2$ ($6 \leq n \leq 8$). Results for the other measured isotopes, ^{42}Ca , ^{44}Ca , and ^{46}Ca , are omitted from the figure so as to avoid overcrowding.

Although our measurements are not as extensive as our Sr work reported above, it is possible to see that the transition shifts to the high $4sns\ ^1S_0$ states ($9 \leq n \leq 11$) have converged on to a straight line parallel to, but shifted from the BMS. The RLIS presented in Table III are derived from the measured TIS, tabulated in Table II, by using the ground-state RLIS obtained from the 1S_0 series above $n=9$. While this value of the ground-state RLIS has not yet been confirmed by further measurements on a second series converging to the same ionization limit, support for the above procedure comes from the fact that the quantum defect for the three excited 1S_0 states ($9 \leq n \leq 11$) are constant with n , indicating that these states are free of configuration mixing effects.

By contrast, it is clear from Fig. 3 that the $4snd\ ^1D_2$ states have strongly perturbed level isotope shifts. From earlier quantum defect measurements

by Armstrong *et al.*,² it is known that this series is strongly perturbed around $n=8$ by a term ($J=2$) of the $3d\ 5s$ doubly excited configuration. We therefore undertook a measurement of the isotope shift in this perturber state. Figure 4 shows a spectral scan of the transition $4s^2\ ^1S_0$ to the $3d\ 5s$ configuration. The good signal-to-noise ratio in this spectrum is evident from the signal from ^{46}Ca which has a natural abundance of only 33 parts per million.

It can be seen from Fig. 3 that the $3d\ 5s$ perturber state is sufficiently strongly mixed with the $4snd\ ^1D_2$ series that the RLIS of states of the two configurations are of comparable size. As observed for the perturbed 1D series in Sr, we expect the 1D series of isotope shifts in calcium to converge to zero at the ionization limit.

Calcium gives us a special opportunity of extracting separately both the mass and field isotope shifts. Two of its naturally abundant isotopes, ^{40}Ca and ^{48}Ca , have so-called "doubly magic" nuclei, in which both the neutron and proton shells of each nucleus are closed and spherically symmetric. Träger¹⁸ observed that the isotope shifts of the transitions from $4s^2\ ^1S_0$ to the $4s\ 4p\ P$ states had nearly zero field shift between ^{40}Ca and ^{48}Ca , after examination of a King plot. Together with muonic data, Träger deduced that the change in the squared radius of the nucleus between these two isotopes was nearly zero. Within the accuracy of our measurements, which are inferior to those of Träger, this implies that all RLIS between ^{40}Ca and ^{48}Ca are purely specific mass shifts.

We give in Table III the specific mass level shift (SMS) and field level shift (FS) for each Ca level measured. Where earlier measurements by other workers of transition shifts have been made to states relevant to the present work, for example, as part of the $4sns\ ^1S_0$ series, we derive the level shift and include it in Table III. The SMS in the isotope pairs ^{48}Ca - ^{40}Ca are simply derived by scaling the RLIS of ^{48}Ca - ^{40}Ca by the mass factor

$$\left[\frac{A_{48}A_{40}}{A_{48}-A_{40}} \right] \left[\frac{(A_{48}-A_N)}{A_{48}A_N} \right]$$

which is simply the ratio of differences of reduced mass factors between the isotopes of mass A_N . The field shifts are of course derived by subtracting the SMS from the RLIS.

Despite large error bars, it is clear that the specific mass shift is the predominant isotope effect in all observed states of calcium. The perturbed 1D series, for example, has purely specific mass shifts which are, incidentally, an order of magnitude larger than the ground-state shifts. Only the ground state and the first excited P states appear to have field shifts at our level of accuracy. Our level shifts show that

the field shifts in the $4s4p\ ^1P_1$ and $4s4p\ ^3P_1$ states are opposite in sign to those in the $4s^2\ ^1S_0$ ground state, thereby indicating the need to include an account of screening effects in describing the shifts of the excited P states. The field shifts of these lower levels show the odd-even staggering as deduced by Träger¹⁸ from King plots of the transition shifts between these levels, and corresponding to the successive adding of neutrons to the $f_{7/2}$ shell of the calcium nucleus between $^{40}_{20}\text{Ca}$ and $^{48}_{20}\text{Ca}$.

IV. CONCLUSION

The concept of level isotope shifts in optical spectra of atoms is an old one. Yet it has only very occasionally been employed, despite its obvious greater interest to the theoretician than transition shifts which in general are differences of two unknown

numbers. The present work reports, for the first time, level shifts in neutral Ca and Sr, given relative to the ground state of the first ion of each element. The specific mass isotope effect is found to be predominant in the level shifts of these elements, often taking values in highly excited states which are larger than the isotope shifts of the lower levels, when the upper levels are affected by state mixing.

ACKNOWLEDGMENTS

We have benefited from many discussions, especially on the interpretative aspects of this work, with several members of the group at Göteborg, particularly Ann-Marie Mårtensson-Pendrill. Financial support by the Deutsche Forschungsgemeinschaft and the Swedish National Research Council is gratefully acknowledged.

-
- ¹E. W. Otten, Nucl. Phys. A **354**, 471c (1981).
²J. A. Armstrong, P. Esherrick, and J. J. Wynne, Phys. Rev. A **15**, 180 (1977).
³R. Beigang and A. Timmermann, Phys. Rev. A **25**, 1496 (1982).
⁴P. Grundevik, M. Gustavsson, I. Lindgren, G. Olsson, L. Robertsson, A. Rosen, and S. Svanberg, Phys. Rev. Lett. **42**, 1528 (1979).
⁵C. Palmer, P. Baird, J. Nicol, D. Stacey, and K. Woodgate, J. Phys. B **15**, 993 (1982).
⁶R. Ritschl and H. Schober, Phys. Z **38**, 6 (1937).
⁷L. Bradley and H. Kuhn, Proc. R. Soc. London Ser. A **209**, 325 (1951).
⁸K. Niemax and L. R. Pendrill, J. Phys. B **13**, L461 (1980).
⁹A.-M. Mårtensson and S. Salomonson, J. Phys. B **15**, 2115 (1982).
¹⁰C.-J. Lorenzen and K. Niemax, J. Phys. B **15**, L139 (1982).
¹¹W. L. Brillet and A. Gallagher, Phys. Rev. A **22**, 1012 (1980).
¹²C.-J. Lorenzen, K. Niemax, and L. R. Pendrill, Opt. Commun. **39**, 370 (1981).
¹³J. Rubbmark and S. Borgström, Phys. Scr. **18**, 196 (1978).
¹⁴K. Heilig, Z. Phys. **161**, 252 (1961).
¹⁵H. Kopfermann, *Nuclear Moments* (Academic, New York, 1958).
¹⁶R. Beigang, D. Schmidt, and A. Timmermann, J. Phys. B **15**, L201 (1982); R. Beigang, E. Matthias, and A. Timmermann, Phys. Rev. Lett. **47**, 326 (1981); **48**, 290(E) (1982).
¹⁷R. Beigang, K. Lücke, A. Timmermann, P. J. West, and D. Fröhlich, Opt. Commun. **42**, 19 (1982).
¹⁸F. Träger, Z. Phys. A **299**, 33 (1981).
¹⁹H.-W. Brandt, K. Heilig, H. Knöckel, and A. Steudel, Z. Phys. A **288**, 241 (1978).
²⁰E. Bergmann, P. Bopp, C. Dorsch, J. Kowalski, F. Träger, and G. zu Putlitz, Z. Phys. A **294**, 319 (1980).